

## MARINE MICROBIOLOGY

# Oxidation of trimethylamine to trimethylamine *N*-oxide facilitates high hydrostatic pressure tolerance in a generalist bacterial lineage

Qi-Long Qin<sup>1,2\*</sup>, Zhi-Bin Wang<sup>1,3,4\*</sup>, Hai-Nan Su<sup>1</sup>, Xiu-Lan Chen<sup>1,3</sup>, Jie Miao<sup>1</sup>, Xiu-Juan Wang<sup>1</sup>, Chun-Yang Li<sup>2,3</sup>, Xi-Ying Zhang<sup>1,3</sup>, Ping-Yi Li<sup>1</sup>, Min Wang<sup>2</sup>, Jiasong Fang<sup>5</sup>, Ian Lidbury<sup>6</sup>, Weipeng Zhang<sup>2</sup>, Xiao-Hua Zhang<sup>2</sup>, Gui-Peng Yang<sup>7</sup>, Yin Chen<sup>6</sup>, Yu-Zhong Zhang<sup>2,3,8†</sup>

High hydrostatic pressure (HHP) is a characteristic environmental factor of the deep ocean. However, it remains unclear how piezotolerant bacteria adapt to HHP. Here, we identify a two-step metabolic pathway to cope with HHP stress in a piezotolerant bacterium. *Myroides profundus* D25<sup>T</sup>, obtained from a deep-sea sediment, can take up trimethylamine (TMA) through a previously unidentified TMA transporter, TmaT, and oxidize intracellular TMA into trimethylamine *N*-oxide (TMAO) by a TMA monooxygenase, *MpTmm*. The produced TMAO is accumulated in the cell, functioning as a piezolyte, improving both growth and survival at HHP. The function of the TmaT-*MpTmm* pathway was further confirmed by introducing it into *Escherichia coli* and *Bacillus subtilis*. Encoded TmaT-like and *MpTmm*-like sequences extensively exist in marine metagenomes, and other marine Bacteroidetes bacteria containing genes encoding TmaT-like and *MpTmm*-like proteins also have improved HHP tolerance in the presence of TMA, implying the universality of this HHP tolerance strategy in marine Bacteroidetes.

## INTRODUCTION

The deep ocean (with water depth more than 1000 m) biosphere represents one of the largest ecosystems on Earth and breeds a variety of life forms. It is estimated that more than 10<sup>29</sup> microbial cells exist there (1). In addition, a lot of microorganisms passively migrate from surface seawater to deep seawater every day with marine snow, whale falls, and ocean currents (2, 3). The migration of these microorganisms is accompanied by increasing pressure and decreasing temperature. High hydrostatic pressure (HHP) has a large inhibitory effect on many physiological activities of microbial cells (4), such as membrane fluidity, RNA synthesis, motility, nutrient uptake, cell division, protein synthesis, and replication (5, 6). While many of the sinking microbes are eliminated because of their failure to adapt to the deep-sea environment, no doubt some microbes can survive in deep sea and even grow and reproduce at HHP environment. On the basis of their hydrostatic pressure tolerance ability, bacteria are divided into piezosensitive bacteria, piezotolerant bacteria, piezophiles, and hyperpiezophiles (7). Among them, some piezophiles have been well studied, which are mainly distributed in  $\alpha$ -proteobacteria,  $\delta$ -proteobacteria, and  $\gamma$ -proteobacteria (7, 8). In piezophiles of the family Vibrionaceae, the ToxR/ToxS two-component system is a pressure sensor, which controls the expression of the

*ompH/ompL* genes and many others (4, 9). However, for widely distributed piezotolerant bacteria, it remains unclear whether their adaptation to HHP has driven the evolution of specific gene sets to cope with HHP stress.

Trimethylamine (TMA) and trimethylamine *N*-oxide (TMAO) are nitrogen-containing organic compounds widely dispersed in the ocean. Two functions of TMAO in marine microbes have been described. First, TMAO is used as a nitrogen source by the SAR11 clade and marine Roseobacter clade of  $\alpha$ -proteobacteria (10). Second, TMAO is used as an electron acceptor by some  $\gamma$ -proteobacteria under anaerobic conditions (11), such as *Shewanella* (12–14) and *Vibrio* (11, 15). In addition, the functions of TMAO in marine animals are also studied. One well-known function is related to HHP tolerance of animals in deep sea. Deep-sea animals can enrich TMAO in their cells, which is used to stabilize intracellular proteins and cell structure for their survival under HHP (16). In teleost fish, muscle TMAO contents range from less than 50 mmol/kg in shallow species to more than 260 mmol/kg in a deep-sea species from 4850-m depth (17). It is believed that in the deep ocean with a water depth of more than 5 km, fish cannot survive without TMAO (18). However, it is yet unknown whether deep-sea bacteria use TMAO to cope with HHP stress.

*Myroides profundus* D25<sup>T</sup> (hereafter referred to as strain D25) is a member of the phylum Bacteroidetes, which was isolated from a deep-sea sediment (1245-m water depth) in the southern Okinawa Trough (19). Comparative genomic and transcriptomic analyses have revealed the strategy adopted by this species during its evolution from land to sea (20). In the current study, we found that strain D25 is a piezotolerant bacterium, which uses TMAO as a piezolyte to cope with HHP stress. Strain D25 takes up TMA through a TMA transporter, TmaT, then oxidizes TMA into TMAO using a TMA monooxygenase (*MpTmm*). The resulting accumulation of intracellular TMAO enables growth at high pressure. The function of the TmaT-*MpTmm* pathway was also confirmed by introducing it into *Escherichia coli* and *Bacillus subtilis*. Further analysis showed that

<sup>1</sup>State Key Laboratory of Microbial Technology, Shandong University, Qingdao, China. <sup>2</sup>College of Marine Life Sciences, and Frontiers Science Center for Deep Ocean Multispheres and Earth System, Ocean University of China, Qingdao, China. <sup>3</sup>Laboratory for Marine Biology and Biotechnology, Qingdao National Laboratory for Marine Science and Technology, Qingdao, China. <sup>4</sup>School of Environmental Science and Engineering, Shandong University, Qingdao, China. <sup>5</sup>Shanghai Engineering Research Center of Hadal Science and Technology, College of Marine Sciences, Shanghai Ocean University, Shanghai, China. <sup>6</sup>School of Life Sciences, University of Warwick, Coventry CV4 7AL, UK. <sup>7</sup>Frontiers Science Center for Deep Ocean Multispheres and Earth System, Key Laboratory of Marine Chemistry Theory and Technology, Ministry of Education, Ocean University of China, Qingdao, China. <sup>8</sup>Marine Biotechnology Research Center, State Key Laboratory of Microbial Technology, Shandong University, Qingdao, China.

\*These authors contributed equally to this work.

†Corresponding author. Email: zhangyz@sdu.edu.cn

the presence of TMA also improved the growth of other bacteria in the phylum Bacteroidetes containing genes encoding the TmaT and *MpTmm* homologs under HHP, suggesting that this may be a common strategy adopted by deep-sea Bacteroidetes. This study reveals a new function of TMA/TMAO in marine bacteria and provides a direct link between a unique metabolic pathway and HHP adaptation in deep-sea bacteria.

## RESULTS

### Accumulation of intracellular TMAO facilitates the survival of strain D25 under HHP

Quaternary amines TMA and TMAO are widespread in the ocean, which can be taken up and metabolized as nutrients by marine bacteria of the Roseobacter clade, e.g., *Ruegeria pomeroyi* (21). A gene (MPR\_3295, *Mptmm*) in the genome of strain D25 was predicted to encode a putative TMA monooxygenase (Tmm). Tmm has been reported to convert TMA to TMAO in cosmopolitan marine bacteria such as members of the Roseobacter clade (e.g., *R. pomeroyi*) and the SAR11 clade (*Pelagibacter ubique*), which is essential for the utilization of TMA as a nutrient source in bacteria (21). To test whether it can use TMA or TMAO, strain D25 was cultured with TMA or TMAO as the sole nitrogen source, and *R. pomeroyi* DSS-3 (hereafter referred to as strain DSS-3) was used as a positive control. Unlike strain DSS-3 that could grow with TMA or TMAO as nitrogen source, strain D25 could not grow with either TMA or TMAO as nitrogen source (Fig. 1A). However, when strain D25 was cultured in a 2216E medium containing TMA, it was found that TMA was consumed and TMAO was accumulated intracellularly (Fig. 1B), which suggests that strain D25 can transport TMA into the cell and metabolize TMA into TMAO in the cell but cannot further metabolize TMAO as nutrient. In addition, we searched the genome of strain D25 for genes encoding key enzymes involved in the downstream catabolism of TMAO, i.e., TMAO demethylase (*tdm*) and dimethylamine monooxygenase (*dmmABC*); however, none of such genes were found. This supports our observation that strain D25 cannot metabolize TMAO (Fig. 1B).

Because TMAO is a well-known protein stabilizer that can counteract the effects of HHP in marine animals (18), we postulated that strain D25 may accumulate TMAO in the cell to cope with HHP stress. To test this postulation, we investigated the growth of strain D25 with or without TMA in the medium at the atmospheric pressure, 20 and 40 MPa. The result showed that the addition of TMA in the culture medium improved the growth of strain D25 at 20 MPa and the survival of strain D25 at 40 MPa, and 10  $\mu$ M TMA showed the best effect, but such an effect was not observed at the atmospheric pressure (Fig. 1C and fig. S1A). We then investigated the growth and survival of strain D25 under different HHP conditions and found that the presence of 10  $\mu$ M TMA significantly improved the growth of strain D25 under 10 to 30 MPa and increased the survival of strain D25 even under 50 MPa (Fig. 1D). In contrast, neither TMAO nor any other quaternary amines added in the medium could improve the growth of strain D25 at HHP condition (Fig. 1D and fig. S1B). In these experiments, after incubation of strain D25 under different pressures, the remained dissolved oxygen concentration in the medium was all more than 4.1 mg/liter, indicating that dissolved oxygen was sufficient to support the growth of strain D25 during cultivation and that HHP was the main factor to impair the cell growth. In addition, it is noteworthy that

the presence of TMA also helped maintain the cell integrity and prevent cells from collapsing at 40 MPa (Fig. 1E). Together, these results suggest that strain D25 can take up TMA from the environment and accumulate TMAO in the cell to cope with HHP stress.

### Identification and characterization of the TMA monooxygenase responsible for oxidizing TMA into TMAO in strain D25

Because strain D25 can convert TMA into TMAO in its cell, we speculate that the putative Tmm encoded by the gene *Mptmm* (MPR\_3295) may catalyze this reaction in strain D25. This putative Tmm has 55% sequence identity and 98% sequence coverage with the Tmm of strain DSS-3. To analyze the function of gene *Mptmm*, we overexpressed this gene in *E. coli* BL21 (fig. S2A), and the recombinant protein was active to oxidize TMA into TMAO at both 25° and 4°C (Fig. 2A), indicating that gene *Mptmm* encodes a Tmm, named *MpTmm*. Moreover, the presence of TMA in the culture medium significantly induced the transcription of gene *Mptmm* (Fig. 2B), suggesting that gene *Mptmm* is functional in converting TMA to TMAO in strain D25. HHP also induced the higher expression level of gene *Mptmm* in strain D25 (Fig. 2C), suggesting that gene *Mptmm* may be involved in coping with HHP stress in strain D25.

We further characterized the *MpTmm* of strain D25 using the recombinant protein. The crystal structure of *MpTmm* was solved to 1.69 Å (table S1). The overall structure of *MpTmm* is similar to that of *RnTmm* (22), an *MpTmm* homolog from *Roseovarius nubinhibens* ISM (hereafter referred to as strain ISM), with a root mean square deviation between these two structures of 0.8 Å (Fig. 2D). The cofactors flavin adenine dinucleotide (FAD) and nicotinamide adenine dinucleotide phosphate (NADP<sup>+</sup>) in these two structures are also located in the similar positions (Fig. 2E). In addition, *MpTmm* has 52.8% sequence identity and 98% sequence coverage with *RnTmm*. These data further indicate that *MpTmm* is a Tmm. Strain ISM is a marine Roseobacter clade strain isolated from the surface water of the Caribbean Sea (23). Compared with *RnTmm* (22), *MpTmm* displays typical characteristics of a cold-adapted enzyme. It has a low optimum temperature of 25°C, retains 20 to 40% of the maximum activity at 0° to 5°C (Fig. 2F), and has a low  $T_m$  (denaturing temperature) of 42° ± 0.05°C (Fig. 2G). In addition, even at 50 MPa pressure, *MpTmm* still retained 59% (25°C) and 43% (4°C) of its activity at atmosphere pressure (Fig. 2H). Together, these results indicate that *MpTmm* is a cold-adapted and HHP tolerant enzyme, which can be functional in the in situ deep-sea environment with low temperature and high pressure. Thus, it can be predicted that strain D25 is capable of converting TMA into TMAO via *MpTmm* and accumulating TMAO in its cell in the in situ deep-sea environment.

### Identification and characterization of the TMA-specific transporter in strain D25

The result in Fig. 1B showed that TMA in the 2216E medium of strain D25 was consumed during cultivation, indicating that strain D25 can transport TMA into its cell. We tried to find the gene encoding the TMA transporter by searching the genome of strain D25, but failed. Then, we sequenced the transcriptomes of strain D25 cultured under different pressures to uncover the potential TMA transporter and to investigate the expression and regulation of the genes involved in TMA metabolism. When the pressure increased, there are 533 and 430 genes significantly up- and down-regulated,

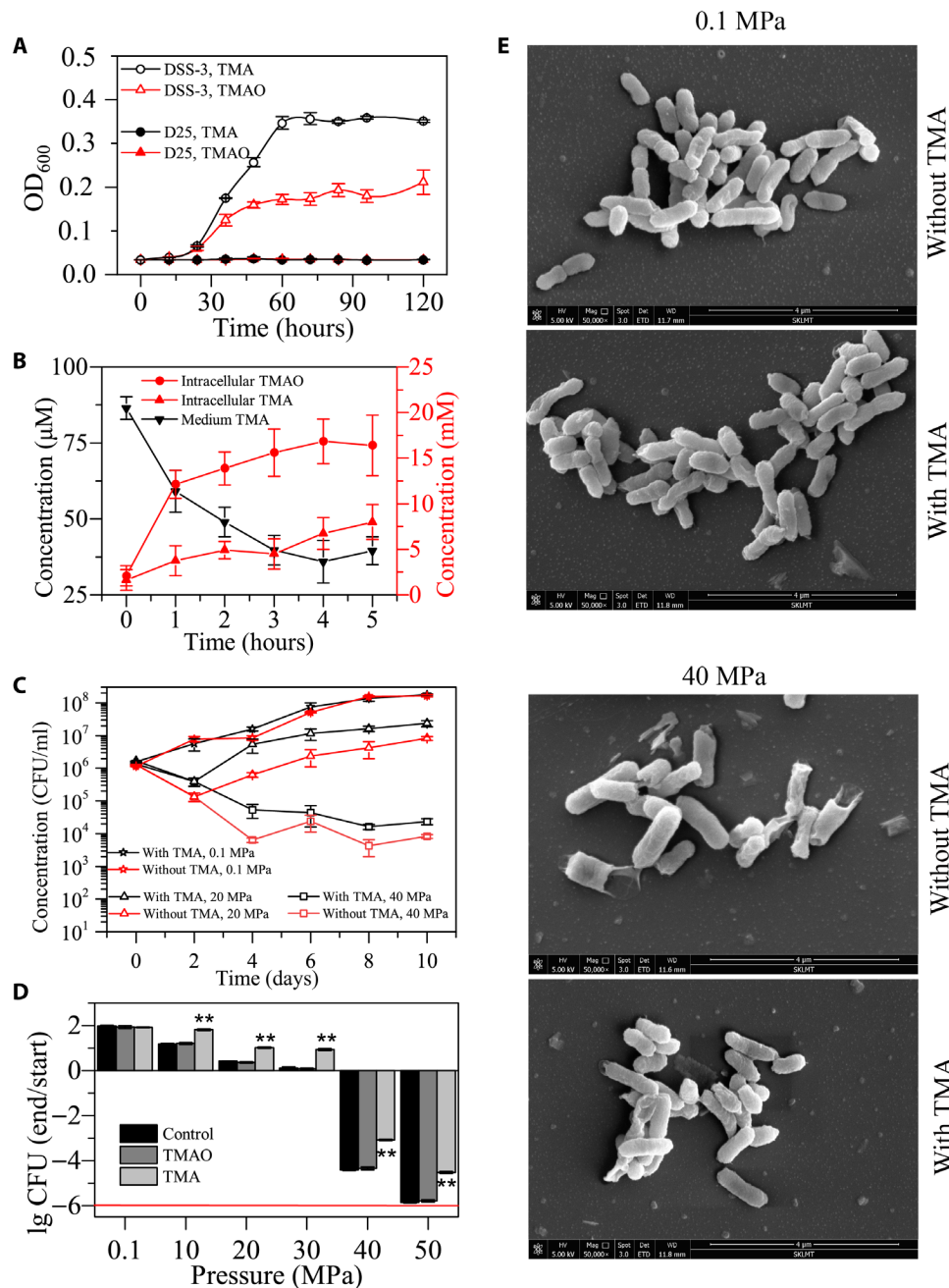


**Fig. 1. Effect of methylamine on the growth and survival of strain D25 under HHP.** (A) Growth curves of strains D25 and DSS-3 cultured with TMA or TMAO as the sole nitrogen source. (B) Changes of the concentrations of medium TMA and intracellular TMA and TMAO of strain D25 cultured in 2216E medium with an initial TMA concentration of 85  $\mu\text{M}$ . (C) Growth curves of strain D25 at 4°C at 0.1, 20, and 40 MPa with or without 10  $\mu\text{M}$  TMA. (D) Effect of 10  $\mu\text{M}$  TMAO or TMA on the growth and survival of strain D25 at different pressures. The cell number at the start of the incubation (start) was ca.  $1 \times 10^6$  CFU/ml. The cultures were incubated at 4°C for 10 days, and then CFU was counted and compared with that of the starting culture (end/start). The red line refers to a complete death of cells in the culture. Control: Strain D25 cultured without TMAO or TMA. (E) Morphological observation of strain D25 cultivated at different pressures with or without 10  $\mu\text{M}$  TMA. The error bars represent SDs from triplicate experiments. The asterisks show statistical difference from control (\*\* $P < 0.01$ , two-tailed  $t$  test). ETD, Everhart-Thornley detector; WD, working distance. SKLMT, State Key Laboratory of Microbial Technology.

respectively, and the transcription level of the gene *Mptmm* was up-regulated 22.2-fold, consistent with the result in Fig. 2C. We then screened the transporter genes whose transcription levels were up-regulated at HHP condition (38 genes were found), and a gene (MPR\_0426, *tmaT*) encoding a predicted membrane protein belonging to the betaine, carnitine, and choline transporter (BCCT) family

was found to be up-regulated 7.9-fold. The quantitative real-time polymerase chain reaction (PCR) result also confirmed that HHP induced higher expression level of this gene (Fig. 3A), suggesting that gene *tmaT* may be involved in coping with HHP stress in strain D25.

Transporters of the BCCT family are responsible for the uptake of several quaternary amines and other organic osmolytes in bacteria,

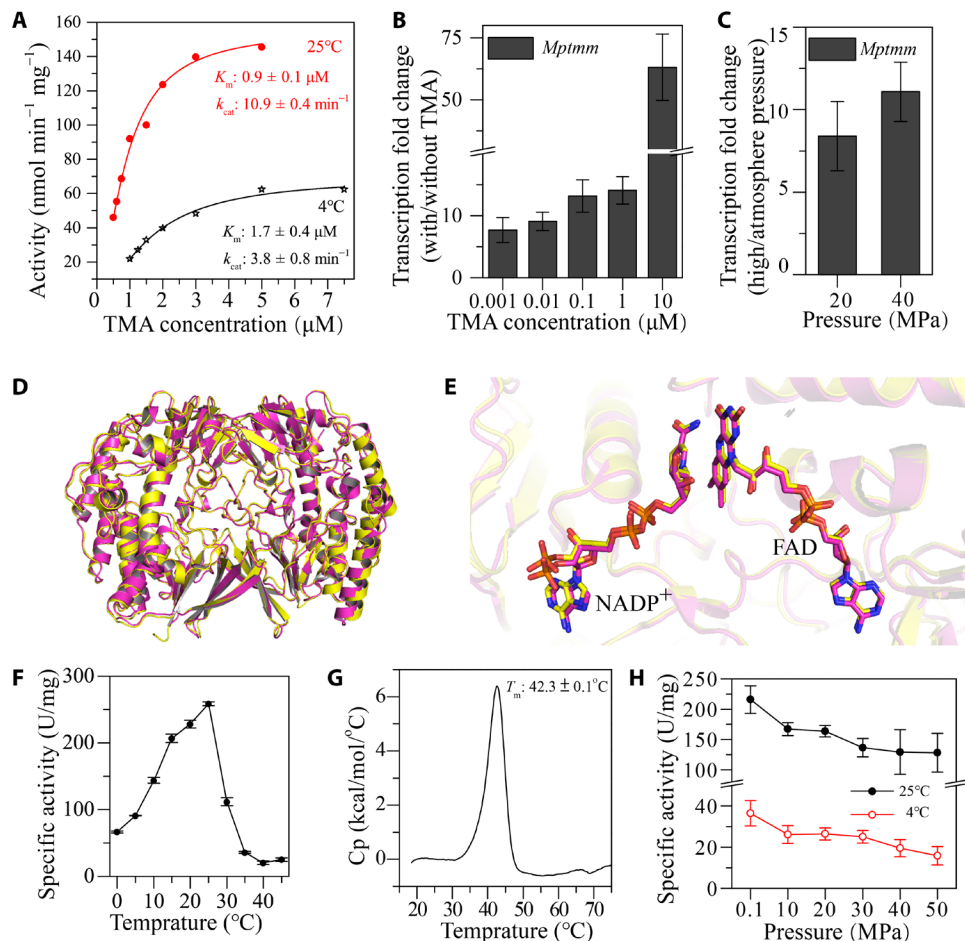


**Fig. 2. Characterization of *MpTmm*.** (A) Nonlinear fit curves for the oxidation of TMA by recombinant *MpTmm* at 4° and 25°C. (B) Effect of different concentrations of TMA on the expression of gene *Mptmm* in strain D25. Strain D25 was cultured in 2216E medium with or without TMA for 1 hour. (C) Effect of hydrostatic pressure on the expression of gene *Mptmm* in strain D25. Strain D25 was cultured in 2216E medium at atmosphere pressure, 20 or 40 MPa for 1 hour. (D) Comparison of the structures of *MpTmm* and *RnTmm*. *MpTmm* is colored in yellow, and *RnTmm* in purple. (E) Comparison of the locations of NADP<sup>+</sup> (left) and FAD (right) in the crystal structures of *MpTmm* and *RnTmm*. The FAD and NADP<sup>+</sup> molecules are shown in sticks colored in yellow for *MpTmm* and in purple for *RnTmm*. (F) Effect of temperature on the activity of *MpTmm*. (G) Measurement of the  $T_m$  value of *MpTmm* by DSC. (H) Effect of pressure on the activity of *MpTmm*. The enzymatic activities at different pressures were measured at 25° and 4°C, respectively. The error bars represent SDs from triplicate experiments.

including glycine betaine, choline, carnitine, and dimethylsulfoniopropionate (DMSP) (24). To ascertain whether gene *tmaT* encodes a TMA transporter, we overexpressed this gene in *E. coli* BL21 (fig. S2B) and tested the substrate binding specificity of the recombinant protein using isothermal titration calorimetry (ITC) assays. The result showed that the recombinant protein had a high binding affinity to TMA (Fig. 3, B to D) and did not bind TMAO (Fig. 3E), glycine betaine, carnitine, choline, or DMSP (fig. S3), which indicates that gene *tmaT* encodes a TMA-specific transporter, which is named TmaT. Because no TMA transporter has ever been reported, TmaT represents a new member of the BCCT family, which is different in substrate specificity from the other BCCT family proteins including transporters BetP, BetT, and CaiT for glycine betaine, choline, and carnitine, respectively. This is further supported by phylogenetic analysis, which showed that TmaT and its homologs are clustered in a separate branch from the other BCCT family sequences (Fig. 3F). In addition, we found that the dissociation constant ( $K_d$ ) of TmaT for TMA binding at 5°C was lower than that at 15° or 25°C (Fig. 3, B to D), suggesting that TmaT can function well

at deep-sea in situ temperature. Together, these results suggest that TmaT is a TMA-specific transporter, which is likely responsible for TMA uptake from the environment into strain D25 cells.

#### Analysis of the in vivo function of TmaT and *MpTmm* in recombinant *E. coli* and *B. subtilis*

During our study, we made numerous attempts to disrupt the genes *tmaT* and *Mptmm* in strain D25. Unfortunately, all our attempts failed. Alternatively, we tested the function of TmaT and *MpTmm* in vivo in recombinant *E. coli* (strain DH5 $\alpha$ ) in which TmaT and *MpTmm* were constitutively expressed. We investigated whether the introduction of both genes *tmaT* and *Mptmm* can improve the survival and growth of *E. coli* under HHP. As shown in fig. S4A, heterologous expression of TmaT conferred upon *E. coli* the ability to transport exterior TMA into its cells, indicating that TmaT is a functional TMA transporter. Coexpression of both genes *tmaT* and *Mptmm* in *E. coli* resulted in the accumulation of TMAO intracellularly in *E. coli* when TMA was present in the medium (fig. S4B), indicating that TmaT is responsible for TMA uptake and that *MpTmm* is

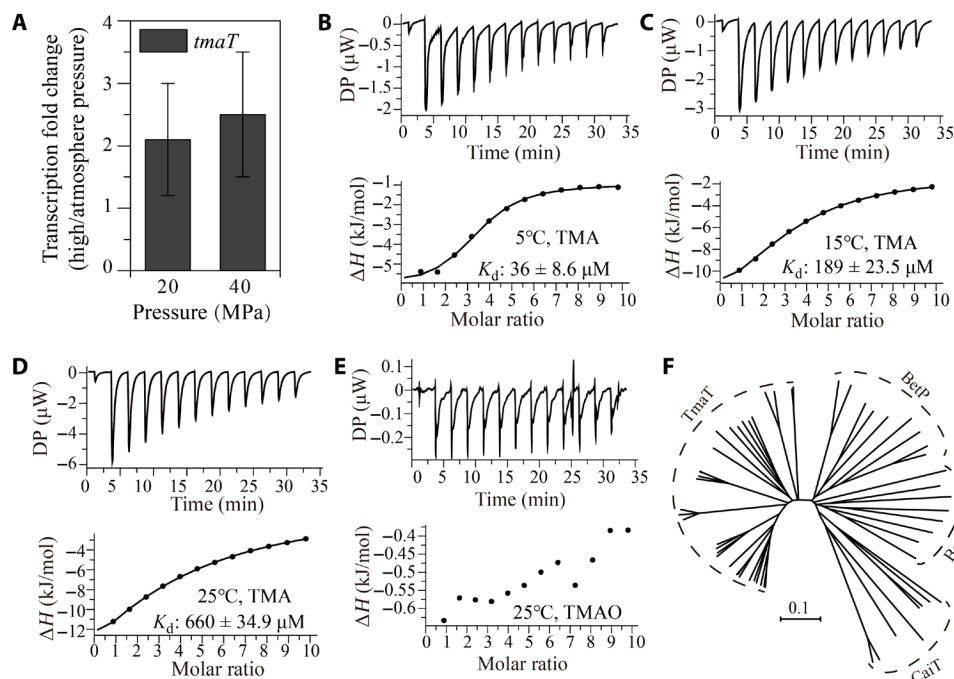


**Fig. 3. Characterization of TmaT.** (A) Effect of hydrostatic pressure on the expression of gene *tmaT* in strain D25 detected by quantitative real-time PCR. Strain D25 was cultured in 2216E medium at atmosphere pressure, 20 or 40 MPa for 1 hour. The error bars represent SDs from triplicate experiments. (B to E) ITC curves for titrations of TMA or TMAO into TmaT. ITC traces (top) and integrated binding isotherms (bottom) are shown. The titration substrates and temperatures are shown in the pictures. DP, differential power. (F) Molecular phylogenetic analysis of TmaT and its homologs with other BCCT transporters. Sequences are from the IMG/JGI database. BetP, BetT, and CaiT are BCCT transporters for glycine betaine, choline, and carnitine, respectively.

responsible for intracellular TMA oxidation to produce TMAO. At the atmospheric pressure, coexpression of both genes did not affect the growth of *E. coli* regardless of whether or not TMA was present (Fig. 4A and fig. S4C). However, coexpression of both genes improved the growth of *E. coli* at HHP conditions (20 and 40 MPa) when TMA was supplied, while expression of TmaT or *MpTmm* alone with addition of TMA, or coexpression of both genes without TMA in the medium, did not improve the growth or survival of *E. coli* at HHP (Fig. 4A and fig. S4C). This indicates that the TMA metabolism involved in TmaT and *MpTmm* in *E. coli* can improve its HHP tolerance.

Because *E. coli* contains a TMAO reductase gene in the *torCAD* cluster (including the genes encoding a pentaheme c-type cytochrome, TMAO reductase, and molecular chaperone) that may further metabolize intracellular TMAO to eliminate the effect of TMAO reductase on the pressure tolerance of the recombinant *E. coli* strain, we knocked out the *torCAD* cluster from *E. coli* and constructed the mutant strain  $\Delta\text{torCAD}$ . The growth of  $\Delta\text{torCAD}$  containing *tmaT* and *MpTmm* at HHP conditions (20 and 40 MPa) was much better than that of the wild-type *E. coli* containing *tmaT* and *MpTmm* when TMA was present in the medium (Fig. 4C and fig. S4D). This further indicates that accumulation of intracellular TMAO is beneficial for *E. coli* to cope with HHP stress.

It has been reported that HHP can impair cell division of *E. coli*, leading to elongated filaments (25, 26). We then investigated the cell morphological changes of  $\Delta\text{torCAD}$  containing genes *tmaT* and *MpTmm* under HHP conditions. When TMA was absent, significantly longer filaments were observed in the cells of  $\Delta\text{torCAD}$  under 20 MPa, and some cells began to collapse under 40 MPa (Fig. 4B). When TMA was present in the medium, coexpression of TmaT and

*MpTmm* reduced the impact of HHP on the cell morphology and cell division of  $\Delta\text{torCAD}$ , especially under 20 MPa (Fig. 4B and fig. S4E).

To further confirm that TmaT and *MpTmm* can improve the HHP tolerant ability of bacteria, the *tmaT* and *MpTmm* genes were introduced into *B. subtilis* 168. As anticipated, the introduction of both genes significantly improved the growth of this strain at HHP conditions (20 and 40 MPa) when TMA was supplied (Fig. 4D and fig. S4F), indicating the improvement of its HHP tolerance.

Overall, these data corroborate the in vivo function of the TMA metabolism pathway mediated by TmaT and *MpTmm* in bacteria, that is, accumulating TMAO to cope with HHP stress. Thus, TMAO, the product of this pathway, is a piezolyte for bacteria.

### Universality of genes *tmaT* and *MpTmm* in marine bacteria

TMA in marine sediments can reach up to 50 μM (27), which is used by sedimentary bacteria. On the basis of the above results, it can be concluded that the deep-sea sedimentary strain D25 can use the environmental TMA to cope with HHP stress via a TMA metabolism pathway mediated by TmaT and *MpTmm*. Strain D25 transports environmental TMA into its cell through the TMA transporter TmaT, and the TMA monooxygenase *MpTmm* oxidizes the intracellular TMA into TMAO, which is accumulated in the cell without further metabolism and used as a piezolyte by strain D25 to cope with HHP stress (Fig. 5A). Thus, the TmaT-*MpTmm* system provides a simple and economic strategy for strain D25 to cope with HHP stress.

To better understand the ecological significance of the TmaT-*MpTmm* system in marine bacteria, genes encoding TmaT-like and *MpTmm*-like proteins were searched in the Integrated Microbial

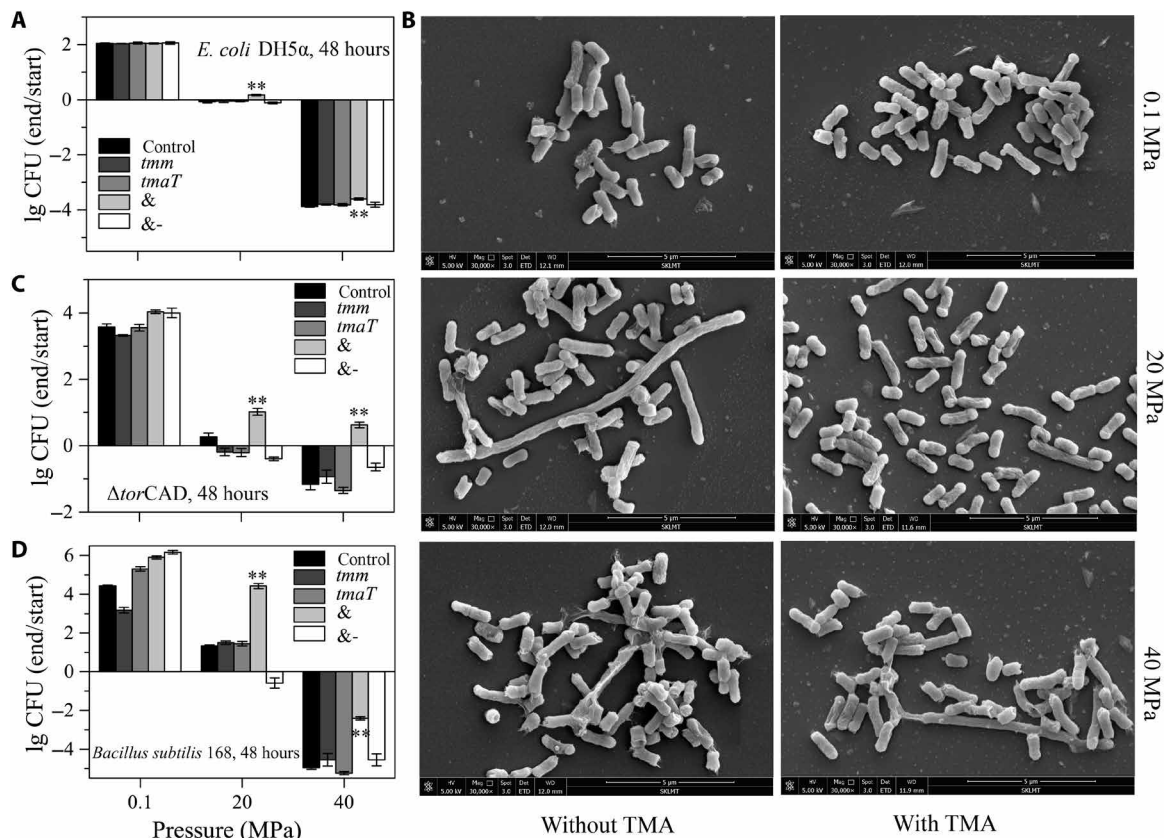


**Fig. 4. The in vivo function of TmaT and MpTmm in recombinant *E. coli* DH5 $\alpha$ , *E. coli* mutant  $\Delta$ *torCAD*, and *B. subtilis* 168. (A, C, and D) Effect of expression of TmaT and MpTmm on the growth and survival of *E. coli* DH5 $\alpha$  (A),  $\Delta$ *torCAD* (C), and *B. subtilis* 168 (D) cultured at different pressures for 48 hours. Control, strain containing the empty plasmid cultured with TMA; *tmm*, strain expressing MpTmm cultured with TMA; *tmaT*, strain expressing TmaT cultured with TMA; &, strain coexpressing MpTmm and TmaT cultured with TMA; and &-, strain coexpressing MpTmm and TmaT cultured without TMA. The cell number at the start of the incubation (start) was ca.  $1 \times 10^5$  CFU/ml. The strains were cultivated at 25°C for 48 hours with or without 20  $\mu$ M TMA, and then CFU were counted and compared with those of the starting culture (end/start). The asterisks show statistical difference from control (\*\* $P < 0.01$ , two-tailed *t* test). The error bars represent SDs from triplicate experiments. (B) Morphological observation of cells of  $\Delta$ *torCAD* coexpressing TmaT and MpTmm cultured at 25°C for 48 hours under different pressures with or without 20  $\mu$ M TMA. ETD, Everhart-Thornley detector; WD, working distance. SKLMT, State Key Laboratory of Microbial Technology.**

Genome Database of the Joint Genome Institute (the IMG/JGI database) (28, 29). TmaT-like and MpTmm-like proteins are found in the marine metagenome dataset (table S2) from many sites across a range of sampling depths, indicating that the two genes are widespread. When we searched the IMG/JGI database with gene *tmaT* as the query, all the *tmaT* homologs (>40% identity) are from Bacteroidetes. Therefore, it is most likely that the TmaT-MpTmm system exists only in Bacteroidetes. We then investigated the distribution of genes encoding TmaT-like and MpTmm-like proteins in the genomes of Bacteroidetes from marine environments, including shallow sea (seawater or sediments from <1000-m depth or depth unreported) and deep sea (seawater or sediments from >1000-m water depth). In the IMG/JGI database, 337 genomes of Bacteroidetes were found from shallow sea, and only 7 from deep sea. Among them, 44 contain both *tmaT* and *MpTmm* homologs, including 41 from shallow sea and 3 from deep sea (table S3). These strains are distributed in four classes of Bacteroidetes (fig. S5), and there does not appear to be a distinct evolutionary lineage within the phylum Bacteroidetes that has this TMA metabolism pathway. The three deep-sea strains are *Zunongwangia profunda* SM-A87 from 1234-m water depth (30), *Pedobacter* sp. SM1810 from 3268-m water depth (31), and *Zunongwangia atlantica* 22II14-10F7 from 2927-m water depth (table S3) (32). We investigated the effect of TMA on the growth and survival of these strains

under 20, 30, and 40 MPa. Consistent with the observation on strain D25, the presence of TMA in the medium significantly improved the growth and survival of all these strains under high pressure (Fig. 5B). Thus, accumulation of TMAO in the cell by assimilating environmental TMA to cope with HHP stress may be a common strategy adopted by deep-sea Bacteroidetes bacteria containing the TmaT-MpTmm system.

In addition, because some Bacteroidetes strains from shallow sea also contain both *tmaT* and *MpTmm* homologs (table S3), we tested the effect of TMA on the growth and survival of three Bacteroidetes strains that originated from surface seawater under 20, 30, and 40 MPa, and the result indicated that exterior TMA can improve the survival and growth of all these strains under HHP (Fig. 5B). This suggests that Bacteroidetes strains containing the TmaT-MpTmm system are likely able to cope with HHP stress when they migrate to deep sea, provided that TMA is present. However, it cannot be excluded that there are other functions of this TMA metabolism pathway in bacteria, especially non-deep-sea bacteria, which needs further study.

## DISCUSSION

TMA and TMAO are ubiquitous in the oceans, and their concentrations range from nanomolar in surface seawater to micromolar in

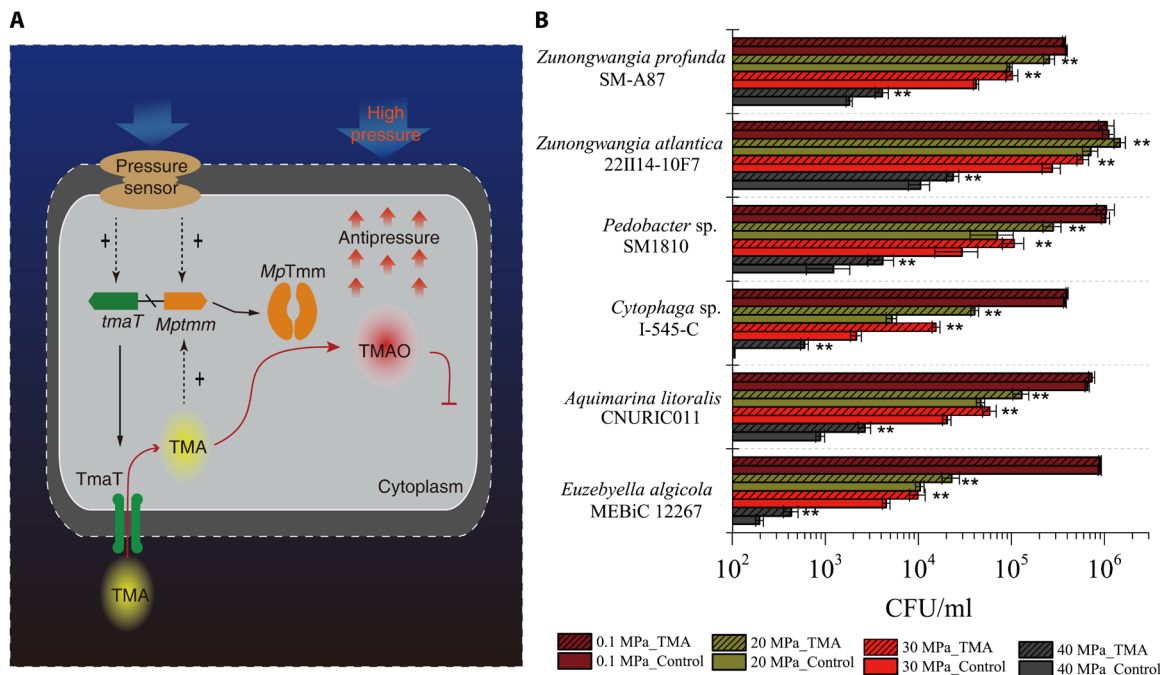


**Fig. 5. The HHP tolerance strategy of strain D25 and its universality in Bacteroidetes.** (A) The proposed model for HHP tolerance of strain D25 via the TMA metabolism pathway mediated by TmaT and MpTmm. Under HHP stress in deep sea, strain D25 expresses genes *tmaT* and *Mptmm* and produces the TMA transporter TmaT and the TMA monooxygenase MpTmm. Strain D25 takes up environmental TMA into its cell by TmaT and oxidizes the intracellular TMA into TMAO by MpTmm. TMAO is accumulated in the cell without further metabolism and is used as a piezolyte by strain D25 to cope with HHP stress. (B) Effect of the presence of TMA in medium on the growth of other Bacteroidetes strains at different pressures. Strains were cultured at 15°C for 10 days in the medium containing 3% artificial sea salt, 0.05% peptone, 0.01% yeast powder, and 20 μM TMA. The error bars represent SDs from triplicate experiments. Strains *E. algicola* MEBiC 12267, *A. litoralis* CNURIC011, and *Cytophaga* sp. I-545-C were all isolated from surface seawater in our lab. The asterisks show statistical difference from control (\*\* $P < 0.01$ , two-tailed  $t$  test). The error bars represent SDs from triplicate experiments.

deep-sea sediments (27), and the content of TMAO in the muscle of deep-sea teleost fish can reach as high as 260 mmol/kg (17). TMA/TMAO metabolism in heterotrophic marine bacteria has been extensively studied over the last decade. On the basis of previous results and the results in this study, it can be concluded that heterotrophic marine bacteria use TMA/TMAO via three pathways (Fig. 6): (i) Many marine  $\alpha$ -proteobacteria including members of the cosmopolitan Roseobacter and SAR11 contain genes *tmm*, *tdm*, and *tmoX* (table S4) and metabolize TMA/TMAO as a carbon, nitrogen, or energy source (10, 27, 33); (ii) some  $\gamma$ -proteobacteria, such as *Shewanella* and *Vibrio*, contain gene *torA* (table S4) and use TMAO as a terminal electron acceptor in anaerobic conditions (13, 15, 34); (iii) and the results in this study reveal that the deep-sea Bacteroidetes strain D25 has a new TMA metabolism pathway mediated by genes *tmaT* and *Mptmm*, which takes up environmental TMA and converts it to TMAO to counteract HHP stress (Figs. 5A and 6). This novel HHP adaptation strategy appears to be nonspecific in strain D25 because heterologous expression of the TmaT-MpTmm system in *E. coli* and *B. subtilis* also leads to their HHP tolerance, and other marine Bacteroidetes bacteria containing genes encoding TmaT-like and MpTmm-like also have improved HHP tolerance in the presence of TMA. Thus, this study uncovers a novel physiological function of TMA/TMAO in marine bacteria and a simple pathway to cope with HHP stress in deep-sea piezotolerant Bacteroidetes bacteria. Bacteroidetes bacteria are widespread in the ocean and considered to play an important role, especially in the degradation of high-molecular weight organic matters in marine ecosystem. This study offers a better understanding of how the generalist

deep-sea bacterial lineage, Bacteroidetes bacteria, survives in deep-sea environments.

## METHODS

### Bacterial strains

Marine bacterial strains *M. profundus* D25, *R. pomeroyi* DSS-3, *E. coli* DH5 $\alpha$ , *E. coli* BL21, *B. subtilis* 168, *Z. profundus* SM-A87, *Pedobacter* sp. SM1810, *Euzebyella algicola* MEBiC 12267, *Aquimarina litoralis* CNURIC011, and *Cytophaga* sp. I-545-C were previously maintained in our lab. *Z. atlantica* 22II14-10F7 was obtained from the Marine Culture Collection of China. The gene knockout mutant of *E. coli* DH5 $\alpha$ ,  $\Delta$ *torCAD*, was constructed as described previously (35). Marine strains D25, DSS-3, SM-A87, SM1810, 22II14-10F7, MEBiC 12267, CNURIC011, and I-545-C were routinely cultivated in the 2216E medium.

### The effect of exterior TMA on the growth of strain D25 at HHP

A defined medium containing 3% (m/v) artificial sea salt, vitamin complex, 1 mM TMA or TMAO, 10 mM glucose, 0.2 mM Na<sub>3</sub>PO<sub>4</sub>, 10 mM HEPES, and 5 μM FeCl<sub>3</sub> (36) was used to test whether TMA or TMAO can be used as a nitrogen source by strains D25 and DSS-3. Automatic growth curve analyzer (Bioscreen C MBR, Finland) was used to record the growth of both strains cultured at 25°C.

To test whether TMA can facilitate the growth of strain D25 at HHP, the medium containing 3% (m/v) artificial sea salt, 0.05% (m/v) peptone, 0.01% (m/v) yeast powder, and TMA (0 to 1 mM) was

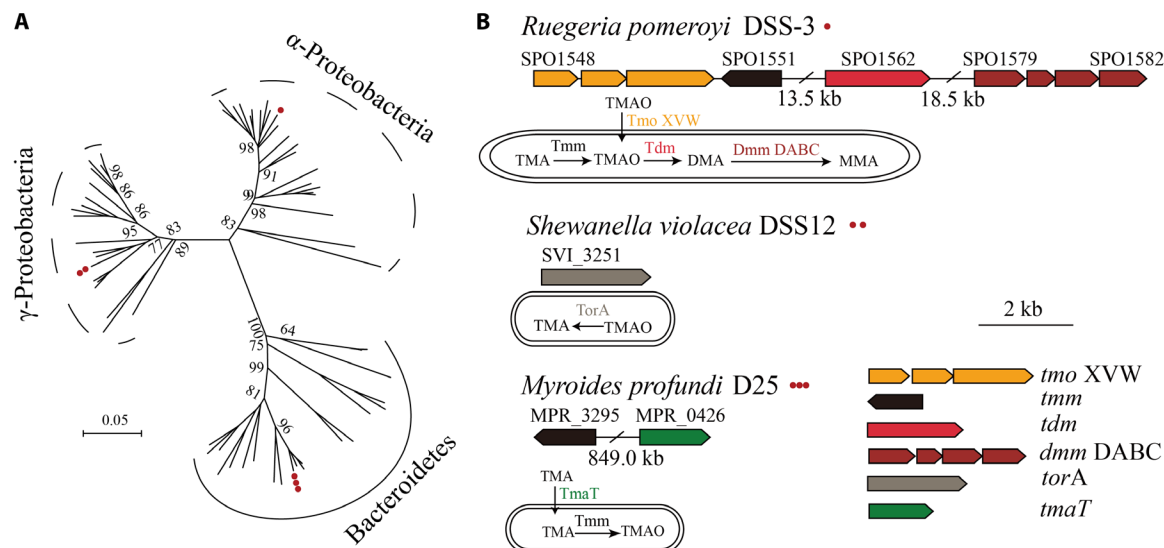


**Fig. 6. Three TMA/TMAO metabolism pathways in marine bacteria.** (A) A neighbor-joining phylogenetic tree showing the bacterial strains, which are capable of metabolizing TMA/TMAO. The tree was constructed on the basis of the 16S ribosomal RNA gene sequences of the strains. The red dot(s) indicates the phylogenetic position of the representative strains illustrated in (B). The detailed information of each strain is listed in table S4. (B) Schemes of the TMA/TMAO metabolism pathways and related genomic regions in *R. pomeroyi* DSS-3 ( $\alpha$ -proteobacteria), *Shewanella violacea* DSS12 ( $\gamma$ -proteobacteria), and *M. profundus* D25 (Bacteroidetes). *MpTmm*, TMA monooxygenase gene; *tdm*, TMAO demethylase gene; *tmaT*, TMA transporter gene; *dmm* DABC, dimethylamine monooxygenase gene; *tmo* XVW, adenosine 5'-triphosphate-dependent TMAO transporter gene; and *torA*, TMAO reductase gene.

used. After 1% (v/v) cell suspension of strain, D25 was inoculated into the medium, 4 ml of culture was filled into a 5-ml sterile syringe with a polyethylene pipe cap, which was then put into the high-pressure vessel, and the hydrostatic pressure was increased to 10, 20, 30, 40, or 50 MPa using a microbial high-pressure culture device (Feiyu Science and Technology Exploitation Co. Ltd., Nantong, China). After incubation at 4°C for 10 days, the syringes were taken out of the high-pressure culture device, and the bacterial cells in each syringe were fully resuspended in the medium by vortexing and shaking. The culture was then diluted using 2216E medium to an appropriate concentration, and 100  $\mu$ l of the diluted culture was plated onto a 2216E agar plate for counting colony-forming units (CFU).

### Scanning electron microscopy imaging

The bacterial cells cultivated at different pressures were collected by centrifugation at 7000g for 3 min. After being fixed with 2.5% (v/v) glutaraldehyde solution, the bacterial cells were washed with ethanol at concentrations of 30, 50, 70, 80, and 90%, respectively, and eventually resuspended in pure ethanol, which were then dried out in Automated Critical Point Dryer (Leica EM CPD300, Germany) with the critical-point drying method and coated with gold using a sputter coater (Cressington 108, England). The surface morphological structures of the bacterial cells were captured in an environmental mode on a scanning electron microscope (FEI Quanta 250 FEG, American) under 5-kV voltage. The length of the bacterial cells was calculated using ImageJ, and Student's *t* test was used to determine the difference in bacterial cell length between different cultivation conditions.

### Quantification of TMA and TMAO

Strain D25 was cultivated at 25°C to an OD<sub>600</sub> (optical density at 600 nm) of ~1.0 in the medium containing 3% (m/v) artificial sea

salt, 0.05% (m/v) peptone, and 0.01% (m/v) yeast powder. Then, a final concentration of 85  $\mu$ M TMA was added into the medium, which was further cultured. Every 1 hour, 1000 ml of culture was centrifuged at 7000g for 3 min, and the supernatant was used for measuring the concentrations of extracellular TMA and TMAO (37). The cell pellet was resuspended in 100 ml of deionized water. After 0.4 M trichloroacetic acid (final concentration) was added, the cells were lysed by sonication. Cell debris was then removed via centrifugation (17,000g, 10 min), and the resultant supernatant was used for measuring the concentrations of intracellular TMA and TMAO. The TMA and TMAO concentrations of all samples were measured on a cation exchange ion chromatograph (ICS-1100, Dionex, USA) with nonsuppressed conductivity detection (38). The optimized eluent solution contained 4 mM nitric acid and 3% (v/v) acetonitrile solution. The separation was carried out on a Metrosep C 4-250/4.0 separation column (Metrohm, Switzerland) under isocratic condition at a flow rate of 0.9 ml/min and a column temperature of 30°C. To determine the intracellular concentrations of TMA/TMAO, the average volume of a cell was first calculated by measuring the average length and diameter of the bacterial cells based on scanning electron microscope observation, assuming a cylinder shape of each bacterial cell. The total volume of the cells in a sample was calculated on the basis of the cell number.

### Transcriptome analysis and quantitative real-time PCR

Strain D25 was cultivated in the 2216E medium to an OD<sub>600</sub> of 0.6 at atmospheric pressure. The culture was then divided into two aliquots and incubated at 30 MPa and atmospheric pressure, respectively, for 1 hour. The cells were collected by centrifugation, and the total RNA was extracted using an RNeasy Protect Bacteria Mini Kit (QIAGEN, Germany). The transcriptome sequencing was performed by Majorbio Co. Ltd. (Shanghai, China), and the reads were mapped to the genome of strain D25. Gene expression was normalized



using the RPKM (reads per kilobases per million mapped reads) method, and the RPKM value of each gene was used to compare levels of expression under different conditions. A gene was considered to be differentially regulated when it showed a >4-fold change in expression and displayed a false discovery rate-adjusted *P* value of <0.01.

For quantitative real-time PCR, DNA-free RNA was reverse transcribed into cDNA by using TransScript First-Strand cDNA Synthesis SuperMix (TransGen Biotech, China). The cDNA was used for quantitative PCR analysis using the LightCycler 1.5 system (Roche, Switzerland), and SYBR Green fluorescence (Takara, Japan) was used for detection. The relative expression of the target gene was normalized to the reference gene of *recA* that was not regulated by HHP.

### Analysis of the in vivo function of TmaT and MpTmm

To analyze the in vivo function of TmaT and MpTmm, recombinant *E. coli* DH5 $\alpha$  mutant strain  $\Delta$ torCAD and strain *B. subtilis* 168 that can constitutively express genes *tmaT* and *Mptmm* were constructed. The genes *Mptmm* and *tmaT* were amplified from the genome DNA of strain D25. BBa-J23111 (<http://parts.igem.org>), a constitutive expression promoter, was introduced in the front primer. The gene *Mptmm* or *tmaT* was recombined with the plasmid pET-22b, and the recombinant plasmid was transformed into  $\Delta$ torCAD and *B. subtilis* 168 by electroporation to construct the MpTmm expression strain and the TmaT expression strain. To construct an MpTmm-TmaT coexpression strain, the gene *Mptmm* was recombined into the TmaT expression plasmid, which was then transformed into  $\Delta$ torCAD and *B. subtilis* 168.

To test the in vivo function of TmaT, the  $\Delta$ torCAD strain containing a TmaT expression plasmid and the  $\Delta$ torCAD strain harboring an empty plasmid were, respectively, cultivated in the medium containing 1% (m/v) NaCl, 0.5% (m/v) peptone, and 0.1% (m/v) yeast powder to an OD<sub>600</sub> of ~1.0. The cells were collected by centrifugation and resuspended in the medium containing 1% (m/v) NaCl, 0.05% (m/v) peptone, 0.01% (m/v) yeast powder, and 30  $\mu$ M TMA, which were then incubated at 25°C, and TMA concentration in the medium was measured every 30 min.

To test the in vivo function of the TmaT-MpTmm metabolism pathway, the  $\Delta$ torCAD strain containing a TmaT-MpTmm co-expression plasmid was cultured in 1 liter of medium containing 1% (m/v) NaCl, 0.5% (m/v) peptone, and 0.1% (m/v) yeast powder to an OD<sub>600</sub> of ~1.0. Then, a final concentration of 85  $\mu$ M TMA was added into the medium, which was further cultured. Concentrations of medium TMA and intracellular TMA and TMAO of  $\Delta$ torCAD were measured every 1 hour as described above.

To test whether TMA can improve the HHP tolerance of strains  $\Delta$ torCAD and *B. subtilis* 168 expressing MpTmm and/or TmaT, the medium containing 1% (m/v) NaCl, 0.05% (m/v) peptone, and 0.01% (m/v) yeast powder and 20  $\mu$ M TMA was used. After incubation under atmosphere pressure, 20 or 40 MPa at 25°C for 40 hours, the CFUs of  $\Delta$ torCAD were counted, and the cell morphology was observed using a scanning electron microscope as described above.

### Expression and purification of MpTmm and TmaT of strain D25

The full-length genes *Mptmm* and *tmaT* were amplified from the genome DNA of strain D25 and were cloned into the pET-22b

vector with a C-terminal His tag, respectively, which were then transformed into *E. coli* BL21. The recombinant *E. coli* strains were cultured at 37°C in Luria-Bertani medium to an OD<sub>600</sub> of 0.8 to 1.0 and then incubated at 20°C for 16 hours with 0.5 mM isopropyl  $\beta$ -D-1-thiogalactopyranoside (IPTG) as an inducer. The recombinant MpTmm protein was purified using the method described by Li *et al.* (39). The recombinant TmaT protein was purified by a membrane protein purification method (40).

### Crystallization, data collection, structure determination, and refinement

The purified recombinant MpTmm (10 mg/ml) was mixed with reduced form of NADP (NADPH) (5 mg/ml) and was crystallized at 18°C using the hanging drops vapor diffusion method. The crystals were obtained in a buffer containing 0.1 M magnesium acetate, 0.1 M MES (pH 6.5), and 10% (w/v) polyethylene glycol 10,000. X-ray diffraction data were collected on BL17U1 beamline at the Shanghai Synchrotron Radiation Facility using detector ADSC Quantum 315r (41). The initial diffraction datasets were processed by HKL2000.

The crystals of MpTmm belong to the *P*<sub>2</sub><sub>1</sub><sub>2</sub><sub>1</sub> space group. The crystal structure of MpTmm was determined by molecular replacement using the CCP4 Program Phaser (42) with the crystal structure of RnTmm (Protein Data Bank code: 5IPY) as the search model. The refinement of the structure was performed using Coot (43) and PHENIX (44). All the structure figures were processed using the program PyMOL ([www.pymol.org/](http://www.pymol.org/)).

### ITC measurements

ITC measurements to test the substrate binding specificity of TmaT were performed at 5°, 15°, and 25°C using the MicroCal iTC200 system (GE Healthcare, USA). The sample cell was loaded with 250  $\mu$ l of protein sample (~10  $\mu$ M), and the reference cell was filled with distilled water. The syringe contained 40  $\mu$ l of tested compound (100  $\mu$ M). The proteins and tested compounds were dissolved in the same buffer containing 10 mM tris-HCl (pH 7.0) and 100 mM NaCl. Titrations were carried out by adding 0.4  $\mu$ l of tested compound for the first injection and 3  $\mu$ l for the following 12 injections, with stirring at 800 revolutions per minute.

### Enzyme assay and characterization

The enzymatic activity of MpTmm toward TMA was measured by following the decrease in absorbance at 340 nm of substrate-dependent oxidation of NADPH as described previously (45). To determine the optimal temperature for MpTmm activity, 300  $\mu$ l of buffer containing 10 mM tris-HCl (pH 8.0), 100 mM NaCl, 0.25 mM NADPH, and 1 mM TMA was preincubated at different temperatures (0° to 45°C) for 30 min. After incubation, 1  $\mu$ M MpTmm was added into the buffer, and the mixture was further incubated at different temperatures for 3 min before detection by Multiskan Spectrum (SpectraMax 384 plus, Molecular Devices, America). To determine the optimal pressure for MpTmm activity, 1 ml of the reaction mixture containing 10 mM tris-HCl (pH 8.0), 100 mM NaCl, 0.25 mM NADPH, 1 mM TMA, and 1 nM MpTmm was incubated at different pressures (0.1 to 50 MPa) for 3 hours before detection by Multiskan Spectrum. The control group had the same reaction system, except that MpTmm was not added. One enzyme activity unit was defined as the amount of enzyme required to consume 1 nM NADPH per minute for TMA oxidation. To determine the *K*<sub>m</sub> of MpTmm, substrate (TMA, dimethylamine, dimethyl sulfide, or

monomethylamine) of different concentrations from 500 to 10  $\mu\text{M}$  was used. The  $K_m$  values of *MpTmm* were determined by nonlinear analysis based on the initial rates, and the measurements were performed at the optimal temperature. All enzyme assays were carried out in triplicate.

Differential scanning calorimetry (DSC) measurements were carried out using a MicroCal VP-DSC (GE Healthcare) to measure the  $T_m$  value of *MpTmm*. The sample cell was loaded with 250  $\mu\text{l}$  of *MpTmm* ( $\sim 15 \mu\text{M}$ ), and the reference cell contained distilled water. The temperature was raised from 25° to 90°C at a constant heating rate of 1°C/min.

### Phylogenetic analyses of TmaT

Using the TmaT of strain D25 as the query, a BLASTP ( $E$  value  $1 \times 10^{-50}$ ) search was performed against all genomes in the IMG/JGI database (<https://img.jgi.doe.gov/cgi-bin/m/main.cgi>) (28, 29), and TmaT homologs were retained. Sequences retrieved from the IMG/JGI dataset were aligned with other characterized BCCT transporters and visualized using Molecular Evolutionary Genetics Analysis version 7.0 (MEGA7) (46).

### Distribution of TmaT-like and *MpTmm*-like proteins in marine metagenomes and marine Bacteroidetes genomes

Metagenomes from different water depths were chosen from the IMG/JGI database. Using *MpTmm* and TmaT of strain D25 as the query, BLASTP analysis was performed using a stringency of 30% identity and a cutoff value of  $10^{-50}$ . The number of retrieved sequences for each protein was normalized by dividing the retrieved number by genome size (Gb). The metagenomes used in this study are listed in table S2.

Genomes of Bacteroidetes isolated from deep-sea water and marine sediments in the IMG/JGI database were screened for TmaT-like and *MpTmm*-like sequences using TmaT and *MpTmm* of strain D25 as the query, respectively (28, 29). Marine Bacteroidetes genomes containing both TmaT-like and *MpTmm*-like sequences are listed in table S3.

### Analysis of enzyme genes involved in the metabolism of methylated amines in marine microbial genomes

All available defined marine bacterial genomes in the IMG/JGI database were screened for enzymes catalyzing degradation of methylated amines using BLASTP analysis with *MpTmm* and TmaT from strain D25, Tdm (Spo1562), and TmoX (Spo1548) from *R. pomeroyi* DSS-3, and TorA (swp\_5031) from *Shewanella piezotolerans* WP3 as query sequences using a stringent cutoff value of  $10^{-50}$ . Marine bacterial genomes containing genes encoding these proteins are listed in table S4. A phylogenetic tree was constructed by a maximum likelihood approach with 500 bootstrap replicates and using a maximum parsimony tree derived from neighbor joining as the initial tree.

### SUPPLEMENTARY MATERIALS

Supplementary material for this article is available at <http://advances.sciencemag.org/cgi/content/full/7/13/eabf9941/DC1>

[View/request a protocol for this paper from Bio-protocol.](#)

### REFERENCES AND NOTES

- J. Kallmeyer, R. Pockalny, R. R. Adhikari, D. C. Smith, S. D'Hondt, Global distribution of microbial abundance and biomass in seafloor sediment. *Proc. Natl. Acad. Sci. U.S.A.* **109**, 16213–16216 (2012).
- L. Lundsten, K. L. Schlining, K. Frasier, S. B. Johnson, L. A. Kuhnz, J. B. J. Harvey, G. Clague, R. C. Vrijenhoek, Time-series analysis of six whale-fall communities in Monterey Canyon, California, USA. *Deep Sea Res. Part I Oceanogr. Res. Papers* **57**, 1573–1584 (2010).
- C. R. Newell, C. H. Pilskaln, S. M. Robinson, B. A. MacDonald, The contribution of marine snow to the particle food supply of the benthic suspension feeder, *Mytilus edulis*. *J. Exp. Mar. Biol. Ecol.* **321**, 109–124 (2005).
- P. M. Oger, M. Jebbar, The many ways of coping with pressure. *Res. Microbiol.* **161**, 799–809 (2010).
- M. Jebbar, B. Franzetti, E. Girard, P. Oger, Microbial diversity and adaptation to high hydrostatic pressure in deep-sea hydrothermal vents prokaryotes. *Extremophiles* **19**, 721–740 (2015).
- Y. Zhang, X. Li, D. H. Bartlett, X. Xiao, Current developments in marine microbiology: High-pressure biotechnology and the genetic engineering of piezophiles. *Curr. Opin. Biotechnol.* **33**, 157–164 (2015).
- J. Fang, L. Zhang, D. A. Bazylinski, Deep-sea piezosphere and piezophiles: Geomicrobiology and biogeochemistry. *Trends Microbiol.* **18**, 413–422 (2010).
- F. M. Lauro, D. H. Bartlett, Prokaryotic lifestyles in deep sea habitats. *Extremophiles* **12**, 15–25 (2008).
- T. J. Welch, D. H. Bartlett, Isolation and characterization of the structural gene for OmpL, a pressure-regulated porin-like protein from the deep-sea bacterium *Photobacterium* species strain 5S9. *J. Bacteriol.* **178**, 5027–5031 (1996).
- I. Lidbury, M. A. Mausz, D. J. Scanlan, Y. Chen, Identification of dimethylamine monooxygenase in marine bacteria reveals a metabolic bottleneck in the methylated amine degradation pathway. *ISME J.* **11**, 1592–1601 (2017).
- L. M. Proctor, R. P. Gunsalus, Anaerobic respiratory growth of *Vibrio harveyi*, *Vibrio fischeri* and *Photobacterium leiognathi* with trimethylamine N-oxide, nitrate and fumarate: Ecological implications. *Environ. Microbiol.* **2**, 399–406 (2000).
- J. P. Dos Santos, C. Iobbi-Nivol, C. Couillault, G. Giordano, V. Méjean, Molecular analysis of the trimethylamine N-oxide (TMAO) reductase respiratory system from a *Shewanella* species. *J. Mol. Biol.* **284**, 421–433 (1998).
- O. N. Lemaire, F. A. Honoré, C. Jourlin-Castelli, V. Méjean, M. Fons, C. Iobbi-Nivol, Efficient respiration on TMAO requires TorD and TorE auxiliary proteins in *Shewanella oneidensis*. *Res. Microbiol.* **167**, 630–637 (2016).
- S. Tranier, I. Mortier-Barrière, M. Ilbert, C. Birck, C. Iobbi-Nivol, V. Méjean, J.-P. Samama, Characterization and multiple molecular forms of TorD from *Shewanella massilia*, the putative chaperone of the molybdoenzyme TorA. *Protein Sci.* **11**, 2148–2157 (2002).
- Q.-J. Yin, W.-J. Zhang, X.-Q. Qi, S.-D. Zhang, T. Jiang, X.-G. Li, Y. Chen, C.-L. Santini, H. Zhou, I.-M. Chou, L.-F. Wu, High hydrostatic pressure inducible trimethylamine N-oxide reductase improves the pressure tolerance of piezosensitive bacteria *Vibrio fluvialis*. *Front. Microbiol.* **8**, 2646 (2018).
- P. H. Yancey, W. R. Blake, J. Conley, Unusual organic osmolytes in deep-sea animals: Adaptations to hydrostatic pressure and other perturbants. *Comp. Biochem. Physiol. A* **133**, 667–676 (2002).
- A. L. Samerotte, J. C. Drazen, G. L. Brand, B. A. Seibel, P. H. Yancey, Correlation of trimethylamine oxide and habitat depth within and among species of teleost fish: An analysis of causation. *Physiol. Biochem. Zool.* **80**, 197–208 (2007).
- P. H. Yancey, M. E. Gerringer, J. C. Drazen, A. A. Rowden, A. Jamieson, Marine fish may be biochemically constrained from inhabiting the deepest ocean depths. *Proc. Natl. Acad. Sci. U.S.A.* **111**, 4461–4465 (2014).
- X.-Y. Zhang, Y.-J. Zhang, X.-L. Chen, Q.-L. Qin, D.-L. Zhao, T.-G. Li, H.-Y. Dang, Y.-Z. Zhang, *Myroides profundus* sp. nov., isolated from deep-sea sediment of the southern Okinawa Trough. *FEMS Microbiol. Lett.* **287**, 108–112 (2008).
- Y.-Z. Zhang, Y. Li, B.-B. Xie, X.-L. Chen, Q.-Q. Yao, X.-Y. Zhang, M. L. Kempfer, J. Zhou, A. Oren, Q.-L. Qin, Nascent genomic evolution and allopatric speciation of *Myroides profundus* D25 in its transition from land to ocean. *MBio* **7**, e01946-15 (2016).
- Y. Chen, N. A. Patel, A. Crombie, J. H. Scrivens, J. C. Murrell, Bacterial flavin-containing monooxygenase is trimethylamine monooxygenase. *Proc. Natl. Acad. Sci. U.S.A.* **108**, 17791–17796 (2011).
- C.-Y. Li, X.-L. Chen, D. Zhang, P. Wang, Q. Sheng, M. Peng, B.-B. Xie, Q.-L. Qin, P.-Y. Li, X.-Y. Zhang, H.-N. Su, X.-Y. Song, M. Shi, B.-C. Zhou, L.-Y. Xun, Y. Chen, Y.-Z. Zhang, Structural mechanism for bacterial oxidation of oceanic trimethylamine into trimethylamine N-oxide. *Mol. Microbiol.* **103**, 992–1003 (2017).
- J. M. González, J. S. Covert, W. B. Whitman, J. R. Henriksen, F. Mayer, B. Scharf, R. Schmitt, A. Buchan, J. A. Fuhrman, R. P. Kiene, M. A. Moran, *Silicibacter pomeroyi* sp. nov. and *Roseovarius nubinhibens* sp. nov., dimethylsulfoniopropionate-demethylating bacteria from marine environments. *Int. J. Syst. Evol. Microbiol.* **53**, 1261–1269 (2003).
- C. Ziegler, E. Bremer, R. Krämer, The BCCT family of carriers: From physiology to crystal structure. *Mol. Microbiol.* **78**, 13–34 (2010).
- T. J. Welch, A. Farewell, F. C. Neidhardt, D. H. Bartlett, Stress response of *Escherichia coli* to elevated hydrostatic pressure. *J. Bacteriol.* **175**, 7170–7177 (1993).

26. S. L. Black, A. Dawson, F. B. Ward, R. J. Allen, Genes required for growth at high hydrostatic pressure in *Escherichia coli* K-12 identified by genome-wide screening. *PLoS ONE* **8**, e73995 (2013).
27. J. Sun, M. A. Mausz, Y. Chen, S. J. Giovannoni, Microbial trimethylamine metabolism in marine environments. *Environ. Microbiol.* **21**, 513–520 (2019).
28. I.-M. A. Chen, K. Chu, K. Palaniappan, M. Pillay, A. Ratner, J. Huang, M. Huntemann, N. Varghese, J. R. White, R. Seshadri, T. Smirnova, E. Kirtson, S. P. Jungbluth, T. Woyke, E. A. Elloe-Fadrosh, N. N. Ivanova, N. C. Kyrpides, IMG/M v.5.0: An integrated data management and comparative analysis system for microbial genomes and microbiomes. *Nucleic Acids Res.* **47**, D666–D677 (2019).
29. S. Mukherjee, D. Stamatidis, J. Bertsch, G. Ovchinnikova, H. Y. Katta, A. Mojica, I.-M. A. Chen, N. C. Kyrpides, T. Reddy, Genomes OnLine database (GOLD) v.7: Updates and new features. *Nucleic Acids Res.* **47**, D649–D659 (2019).
30. Q.-L. Qin, X.-Y. Zhang, X.-M. Wang, G.-M. Liu, X.-L. Chen, B.-B. Xie, H.-Y. Dang, B.-C. Zhou, J. Yu, Y.-Z. Zhang, The complete genome of *Zunongwangia profunda* SM-A87 reveals its adaptation to the deep-sea environment and ecological role in sedimentary organic nitrogen degradation. *BMC Genomics* **11**, 247 (2010).
31. X.-y. He, N. Li, X.-l. Chen, Y.-z. Zhang, X.-y. Zhang, X.-y. Song, *Pedobacter indicus* sp. nov., isolated from deep-sea sediment. *Antonie Van Leeuwenhoek* **113**, 357–364 (2020).
32. R. Shao, Q. Lai, X. Liu, F. Sun, Y. Du, G. Li, Z. Shao, *Zunongwangia atlantica* sp. nov., isolated from deep-sea water. *Int. J. Syst. Evol. Microbiol.* **64**, 16–20 (2014).
33. I. Lidbury, J. C. Murrell, Y. Chen, Trimethylamine *N*-oxide metabolism by abundant marine heterotrophic bacteria. *Proc. Natl. Acad. Sci. U.S.A.* **111**, 2710–2715 (2014).
34. K.-M. Lee, Y. Park, W. Bari, M. Y. Yoon, J. Go, S. C. Kim, H.-I. Lee, S. S. Yoon, Activation of cholera toxin production by anaerobic respiration of trimethylamine *N*-oxide in *Vibrio cholerae*. *J. Biol. Chem.* **287**, 39742–39752 (2012).
35. Z.-C. Yu, D.-L. Zhao, L.-Y. Ran, Z.-H. Mi, Z.-Y. Wu, X.-P. Pang, X.-Y. Zhang, H.-N. Su, M. Shi, X.-Y. Song, B.-B. Xie, Q.-L. Qin, B.-C. Zhou, X.-L. Chen, Y.-Z. Zhang, Development of a genetic system for the deep-sea psychrophilic bacterium *Pseudoalteromonas* sp. SM9913. *Microb. Cell Fact.* **13**, 13 (2014).
36. Y. Chen, Comparative genomics of methylated amine utilization by marine *Roseobacter* clade bacteria and development of functional gene markers (tmm, gmaS). *Environ. Microbiol.* **14**, 2308–2322 (2012).
37. J. C. Wekell, H. Barnett, New method for analysis of trimethylamine oxide using ferrous sulfate and EDTA. *J. Food Sci.* **56**, 132–135 (1991).
38. M. E. Erupe, A. Liberman-Martin, P. J. Silva, Q. G. J. Malloy, N. Yonis, D. R. Cocker III, K. L. Purvis-Roberts, Determination of methylamines and trimethylamine-*N*-oxide in particulate matter by non-suppressed ion chromatography. *J. Chromatogr. A* **1217**, 2070–2073 (2010).
39. C.-Y. Li, X.-L. Chen, Q.-L. Qin, P. Wang, W.-X. Zhang, B.-B. Xie, H.-N. Su, X.-Y. Zhang, B.-C. Zhou, Y.-Z. Zhang, Structural insights into the multispecific recognition of dipeptides of deep-sea gram-negative bacterium *Pseudoalteromonas* sp. strain SM9913. *J. Bacteriol.* **197**, 1125–1134 (2015).
40. F. Lu, S. Li, Y. Jiang, J. Jiang, H. Fan, G. Lu, D. Deng, S. Dang, X. Zhang, J. Wang, N. Yan, Structure and mechanism of the uracil transporter UraA. *Nature* **472**, 243–246 (2011).
41. Q.-S. Wang, K.-H. Zhang, Y. Cui, Z.-J. Wang, Q.-Y. Pan, K. Liu, B. Sun, H. Zhou, M.-J. Li, Q. Xu, C.-Y. Xu, F. Yu, J.-H. He, Upgrade of macromolecular crystallography beamline BL17U1 at SSRF. *Nucl. Sci. Tech.* **29**, 68 (2018).
42. M. D. Winn, C. C. Ballard, K. D. Cowtan, E. J. Dodson, P. Emsley, P. R. Evans, R. M. Keegan, E. B. Krissinel, A. G. W. Leslie, A. McCoy, S. J. McNicholas, G. N. Murshudov, N. S. Pannu, E. A. Potterton, H. R. Powell, R. J. Read, A. Vagin, K. S. Wilson, Overview of the CCP4 suite and current developments. *Acta Crystallogr. D Biol. Crystallogr.* **67**, 235–242 (2011).
43. P. Emsley, B. Lohkamp, W. G. Scott, K. Cowtan, Features and development of Coot. *Acta Crystallogr. D Struct. Biol.* **66**, 486–501 (2010).
44. P. D. Adams, P. V. Afonine, G. Bunkóczi, V. B. Chen, I. W. Davis, N. Echols, J. J. Headd, L.-W. Hung, G. J. Kapral, R. W. Grosse-Kunstleve, A. J. McCoy, N. W. Moriarty, R. Oeffner, R. J. Read, D. C. Richardson, J. S. Richardson, T. C. Terwilliger, P. H. Zwart, PHENIX: A comprehensive Python-based system for macromolecular structure solution. *Acta Crystallogr. D Biol. Crystallogr.* **66**, 213–221 (2010).
45. A. Alfieri, E. Malito, R. Orru, M. W. Fraaije, A. Mattevi, Revealing the moonlighting role of NADP in the structure of a flavin-containing monooxygenase. *Proc. Natl. Acad. Sci. U.S.A.* **105**, 6572–6577 (2008).
46. S. Kumar, G. Stecher, K. Tamura, MEGA7: Molecular evolutionary genetics analysis version 7.0 for bigger datasets. *Mol. Biol. Evol.* **33**, 1870–1874 (2016).

**Acknowledgments:** We thank the staff from BL18U1 and BL19U1 beamlines of the National Facility for Protein Sciences Shanghai (NFPS) and Shanghai Synchrotron Radiation Facility for assistance during data collection. We also thank C. Sun, Z. Li, S. Wang, H. Yu, X. Zhao, and Y. Guo from State Key laboratory of Microbial Technology of Shandong University for help and guidance in ion chromatography, ITC, DSC, and SEM. **Funding:** This work was supported by the National Natural Science Foundation of China (31870101, U1706207, 31630012, and 91851205), the National Key R&D Program of China (2018YFC1406700), the Program of Shandong for Taishan Scholars (tspd20181203), and the Young Scholars Program of Shandong University (2016WLJH36). **Author contributions:** Q.-L.Q. and Z.-B.W. performed the majority of the experiments and data interpretation. Z.-B.W. and X.-J.W. purified and crystallized the enzyme, and C.-Y.L. solved the structure. H.-N.S. performed the SEM observation. X.-L.C., J.M., P.-Y.L., and X.-Y.Z. helped in the experiments. I.L. and W.Z. performed the bioinformatical analyses. Z.-B.W., J.F., Y.C., and Y.-Z.Z. wrote the manuscript. M.W., X.-H.Z., X.-Y.Z., and G.-P.Y. revised the manuscript. Y.-Z.Z. designed and supervised the study. **Competing interests:** The authors declare that they have no competing interests. **Data and materials availability:** All data needed to evaluate the conclusions in the paper are present in the paper and/or the Supplementary Materials. Additional data related to this paper may be requested from the authors. All the RNA sequencing read data have been deposited in NCBI's Sequence Read Archive (SRA) under project accession number PRJNA540220. The crystal structure of *MpTmm* has been deposited in PDB with the code number of 6KBW.

Submitted 3 December 2020

Accepted 5 February 2021

Published 26 March 2021

10.1126/sciadv.abf9941

**Citation:** Q.-L. Qin, Z.-B. Wang, H.-N. Su, X.-L. Chen, J. Miao, X.-J. Wang, C.-Y. Li, X.-Y. Zhang, P.-Y. Li, M. Wang, J. Fang, I. Lidbury, W. Zhang, X.-H. Zhang, G.-P. Yang, Y. Chen, Y.-Z. Zhang, Oxidation of trimethylamine to trimethylamine *N*-oxide facilitates high hydrostatic pressure tolerance in a generalist bacterial lineage. *Sci. Adv.* **7**, eabf9941 (2021).

## Oxidation of trimethylamine to trimethylamine *N*-oxide facilitates high hydrostatic pressure tolerance in a generalist bacterial lineage

Qi-Long Qin, Zhi-Bin Wang, Hai-Nan Su, Xiu-Lan Chen, Jie Miao, Xiu-Juan Wang, Chun-Yang Li, Xi-Ying Zhang, Ping-Yi Li, Min Wang, Jiasong Fang, Ian Lidbury, Weipeng Zhang, Xiao-Hua Zhang, Gui-Peng Yang, Yin Chen and Yu-Zhong Zhang

*Sci Adv* 7 (13), eabf9941.  
DOI: 10.1126/sciadv.abf9941

### ARTICLE TOOLS

<http://advances.sciencemag.org/content/7/13/eabf9941>

### SUPPLEMENTARY MATERIALS

<http://advances.sciencemag.org/content/suppl/2021/03/22/7.13.eabf9941.DC1>

### REFERENCES

This article cites 46 articles, 10 of which you can access for free  
<http://advances.sciencemag.org/content/7/13/eabf9941#BIBL>

### PERMISSIONS

<http://www.sciencemag.org/help/reprints-and-permissions>

Use of this article is subject to the [Terms of Service](#)

---

*Science Advances* (ISSN 2375-2548) is published by the American Association for the Advancement of Science, 1200 New York Avenue NW, Washington, DC 20005. The title *Science Advances* is a registered trademark of AAAS.

Copyright © 2021 The Authors, some rights reserved; exclusive licensee American Association for the Advancement of Science. No claim to original U.S. Government Works. Distributed under a Creative Commons Attribution NonCommercial License 4.0 (CC BY-NC).